Coloring-Based Inter-WBAN Scheduling for Mobile Wireless Body Area Networks

Shih Heng Cheng, *Student Member*, *IEEE*, and Ching Yao Huang, *Member*, *IEEE*

Abstract—In this study, random incomplete coloring (RIC) with low time-complexity and high spatial reuse is proposed to overcome in-between wireless-body-area-networks (WBAN) interference, which can cause serious throughput degradation and energy waste. Interference-avoidance scheduling of wireless networks can be modeled as a problem of graph coloring. For instance, high spatial-reuse scheduling for a dense sensor network is mapped to high spatial-reuse coloring; fast convergence scheduling for a mobile ad hoc network (MANET) is mapped to low time-complexity coloring. However, for a dense and mobile WBAN, inter-WBAN scheduling (IWS) should simultaneously satisfy both of the following requirements: 1) high spatial-reuse and 2) fast convergence, which are tradeoffs in conventional coloring. By relaxing the coloring rule, the proposed distributed coloring algorithm RIC avoids this tradeoff and satisfies both requirements. Simulation results verify that the proposed coloring algorithm effectively overcomes inter-WBAN interference and invariably supports higher system throughput in various mobile WBAN scenarios compared to conventional colorings.

Index Terms—Wireless body area network, sensors, inter-WBAN interference, scheduling, graph coloring, spatial reuse, time-complexity

1 Introduction

A wireless Body Area Network (WBAN) realizes ubiquitous health monitoring by overcoming the wire-line limitation of conventional near/inner body signal measurements [1], [2]. As illustrated in Fig. 1, a single WBAN can be treated as a "personal sensor network." It is a simple-star network formed by a group of wireless sensor nodes (WSNs) and a central processing node (CPN) that collects various vital signals from these WSNs. However, unlike a sensor network focused on static or low mobility scenarios [3], a WBAN has a higher moving speed and more frequent topology changes due to user movement [2]. The moving topology of multiple WBANs is similar to that of mobile ad hoc networks (MANETs) [4], but with group-based rather than node-based movement. The "high mobility" and "group-based movement" make the WBAN neither equivalent to a sensor network nor to a MANET. A WBAN thus has a high chance of encountering other WBANs, which creates new issues of inter-WBAN scheduling (IWS). Corresponding discussions [5], [6], [7], [8], [9] have just been opened and comprehensive studies are still required.

Distributed interference-avoidance scheduling of wireless networks can be modeled by the notion of distributed graph coloring, which is commonly adopted in sensor networks or MANET [10], [11], [12]. Network topology is modeled as a graph $G = (V, E)$. The vertices V of G represent the wireless nodes; the edges E of G represent radio resource conflicts between mutually interfering node pairs; the color set C in a coloring of G represents the set of distinct resource units (can be time slots, frequency bands, or code sequences). A complete vertex k-coloring of a graph G is a mapping $V(G) \rightarrow C$, where $|C| = k$, such that adjacent vertices receive distinct colors. Thus, interference between wireless nodes can be avoided by mapping different colors (resource units) to adjacent vertices (mutually interfering nodes). A standard message-passing model is adopted in this study. To negotiate the color mapping between vertices, they can have a two-way message exchange with its adjacent vertices. We assume the system is fully synchronous. In other words, all vertices start their coloring algorithms at the same time and execute each step of the algorithm simultaneously. Other terminologies in graph theory refer to [13]. The chromatic number $\chi(G)$ is defined as the minimum k used to completely color graph G; $N(v)$ is defined as the set of adjacent vertices of vertex v; the maximum degree $\Delta(G)$ is defined as the maximum $d(v)$ and $v \in V(G)$, where vertex degree $d(v) = |N(v)|$.

Two basic requirements of IWS are: 1) fast convergence and 2) high channel utilization. In the case of a WBAN user walking on a sidewalk, network topology changes frequently when the user keeps encountering other WBAN users. Therefore, a quick IWS that rapidly detects and responds to every topology change is expected, which could adopt the quick $1 + \Delta(G)$ coloring for MANET [14]. Also, IEEE 802.15 TG6, the standard task group of WBAN, requires that the WBAN protocol should support at least the sensor density: 60 sensors in a 6^3 m^3 space [15]. Such dense WBANs create a high probability of mutual interference. It can significantly decrease the number of coexisting WBAN users due to poor channel utilization [6]. Thus, high channel-utilization IWS is also required, which could adopt an optimal spatial-reuse coloring for dense sensor networks [10]. Optimal spatial-reuse implies

• *The authors are with the Electronics Engineering Department, National Chiao Tung University, 1001 University Rd., Hsinchu City 30010, Taiwan, ROC. E-mail: scott.shcheng.ee95g@g2.nctu.edu.tw, fbil.ee95g@nctu.edu.tw, cyhuang@mail.nctu.edu.tw.*

Manuscript received 12 Aug. 2011; revised 11 Feb. 2012; accepted 12 Apr. 2012; published online 26 Apr. 2012.
Recommended for acceptance by C. Pinotti.
For information on obtaining reprints of this article, please send e-mail to: tpds@computer.org, and reference IEEECS Log Number TPDS-2011-08-0533.
Digital Object Identifier no. 10.1109/TPDS.2012.133.

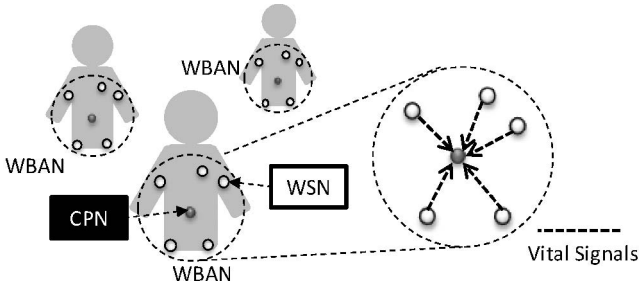

Fig. 1. Wireless body area networks.

the maximal number of sensors that access the wireless channel at the same time.

However, authors in [16], [17], [18] show that quick (low time-complexity) coloring and optimal spatial-reuse coloring are tradeoffs which cannot be simultaneously achieved with conventional complete coloring. Optimal spatial-reuse coloring uses a minimum number of colors, the chromatic number $\chi(G)$, to color a graph. The fewer colors used, the more there is color-reuse among vertices. It implies more wireless nodes can simultaneously transmit packets using the same resource unit, that is, the system has higher spatial-reuse and channel-utilization. However, completely color a graph by using $\chi(G)$ colors is known to be NP-complete. The fastest $\chi(G)$-coloring so far still needs time-complexity $O(2^n n^{O(1)})$ [16]. Nevertheless, study [17] indicates that time-complexity can be significantly reduced to $O(\log n)$ if colors are increased to $1+\Delta(G)$ (sacrificing spatial reuse) and distributed coloring techniques are adopted. $1+\Delta(G) \geq \chi(G)$ is known as Brooks' theorem, which is a loose upper bound for $\chi(G)$. A recent work [19] adopts a similar $1+\Delta(G)$ coloring method. It guarantees not only $O(\log n)$ time-complexity but also $O(\log n)$ bit complexity, which is the amount of information exchanged between vertices during coloring. Low-bit-complexity of a coloring algorithm makes it applicable to low-computing-power applications, such as sensor networks. Although Kothapalli et al. [18] further decrease the time-complexity from $O(\log n)$ to $\tilde{O}(\sqrt{\log n})$[1] by applying vertex priority, $1+\Delta(G)$ colors are still required. As a result, neither $\chi(G)$ [16] nor $1+\Delta(G)$-coloring [17], [18] may be directly applied to IWS due to their high time-complexity and low spatial reuse, respectively.

This paper proposes Random Incomplete Coloring (RIC) to realize quick and high spatial-reuse IWS. RIC consists of 1) a proposed random-value coloring method and 2) an incomplete-coloring approach. The random-value coloring method is a technique which realizes prioritized vertex coloring [18] (so-called oriented coloring) and will be proven to have a low time-complexity $O(e^{W(2\ln n)/2})$,[2] which is even lower than [18]. Besides, for high spatial-reuse coloring, conventional complete coloring using $\chi(G)$ colors is known as the solution for optimal spatial reuse. Surprisingly, for designs of wireless resource scheduling, this study found that higher spatial reuse (on average) than that of $\chi(G)$ coloring is possible if partial vertices are allowed to be uncolored and only $k < \chi(G)$ colors are used. In wireless networks, we observe that uncolored vertices imply wireless nodes with no transmission, which do not interfere each other. Hence, following the nature of wireless communication, there is no conflict between adjacent uncolored vertices (or with the special color: no color). Based on this fact, we can color a subgraph of graph G. This subgraph is constructed using vertices, excluding uncolored ones. Clearly, it is possible to use less colors for the subgraph. For convenience, we name this kind of coloring "incomplete" coloring. The proposed Random Incomplete Coloring will be implemented as an inter-WBAN scheduling protocol with a time-division multiple access (TDMA) framing structure, a common structure used in sensor or body area networks [2], to test its convergence speed and spatial reuse in various mobile WBAN scenarios.

Given $G=(V,E)$; $u,v \in V(G)$; $C_u(r)$ is the set of available colors of u in coloring round r ; The initial size of the available color set is $|C_u(0)| = k = 1+\Delta$; every edge $(u,v) \in E(G)$ has a predefined orientation. For each coloring cycle:

While u is uncolored,

1. u chooses a color c_u from $C_u(r)$.
2. u broadcasts a coloring message with c_u to adjacent vertices in $N(u)$.
3. If u receives coloring messages from $v \in N(u)$ and
   if (**non-oriented coloring**)
   u is colored by c_u only when $c_u \neq c_v$.
   elseif (**oriented coloring**)
   u is colored by c_u when (i) $c_u \neq c_v$ or (ii) $c_u = c_v$ with edge orientation $u \to v$.
   endif
4. if u wins the color, it broadcasts the color taken notification.
5. u removes the colors taken by $N(u)$ from $C_u(r+1)$.

Fig. 2. Oriented and nonoriented colorings (Pri-arts).

The rest of this paper is organized as follows: Section 2 introduces the details of related works and the problem formulation. Section 3 reveals the proposed RIC algorithm. The corresponding analytical models of RIC are provided in Section 4. Section 5 presents the simulation settings and results. Section 6 concludes this paper.

2 Related Works and the WBAN System Model

2.1 Oriented and Nonoriented Coloring

Oriented vertex coloring [18] is a distributed coloring technique that utilizes predefined edge orientation (vertex priority) to improve the coloring speed of (nonoriented) random vertex coloring [17] from $O(\log n)$ to $\tilde{O}(\sqrt{\log n})$. Here, we refer to [17] as nonoriented vertex coloring to distinguish [18] from [17]. The major difference between oriented and nonoriented coloring is the manner of solving color conflicts, as shown in Fig. 2 Step 3. For nonoriented coloring, when color conflict $c_u = c_v$ happens to vertices pair

1. Soft-O: $\tilde{O}(g(n))$ is short for $O(g(n)\log^k g(n))$.
2. $W(x)$ is the Lambert W function [18]. $W(x)$ is solved by inverting the equation, $z = W(z)\exp[W(z)]$, for any complex number z.

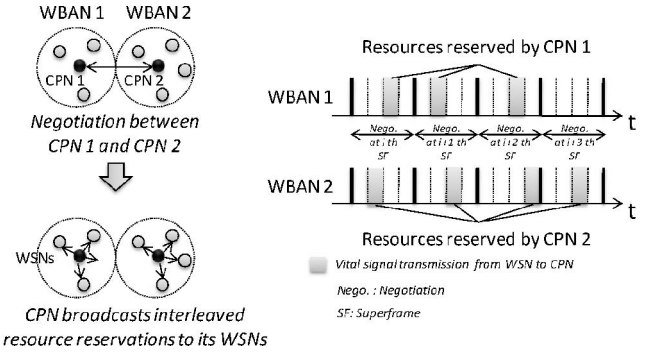

Fig. 3. CPN-based inter-WBAN scheduling.

(u, v), both vertices give up that color and rechoose new colors for the color contention in the next coloring round. In contrast, oriented coloring tries to force the vertex that has a higher priority (having an outward edge orientation) to win the color. Although an oriented conflict path (OCP) may exist ($u \rightarrow v \rightarrow w$, $c_u = c_v = c_w$) and only the vertex u at the start of the path can win the color (no vertex has a higher priority than u has), oriented coloring generates at least one winner for each path in each round (an exception, deadlock circle, will be mentioned later). This is the reason why oriented coloring speeds up coloring.

However, to realize the oriented coloring for IWS, two particular issues need to be considered: 1) fairness and 2) oriented conflict circle (deadlock circle). First, oriented coloring assumes the priorities of vertices are predefined, which is not practical for the dynamic topology of a WBAN. How to dynamically and fairly decide the priority of a WBAN should be further addressed. The second issue is the oriented conflict-circle (deadlock circle) problem. An oriented conflict circle is defined as a circle graph with one-way orientation and vertices in the circle contending for the same color (e.g., $u \rightarrow v \rightarrow w \rightarrow u, c_u = c_v = c_w$). There is no vertex in that circle that can be colored because there is always another adjacent vertex with a higher priority. Thus, the coloring cannot be completed unless vertices try to contend using different colors in subsequent rounds. To solve these two problems, a method that implements oriented coloring, random value coloring, is proposed. Moreover, we will show that this method can further decrease the time-complexity from $\tilde{O}(\sqrt{\log n})$ [18] to $O(e^{W(2\ln n)/2})$.

Aside from the above implementation issues, conventional complete colorings [16], [17], [18], including oriented coloring [18], have an optimum spatial reuse bounded by $\chi(G)$. However, for designs of wireless resource scheduling, spatial reuse can be further improved if the coloring rule is relaxed. The relaxed coloring approach, referred to as incomplete coloring, will be introduced in the next section.

2.2 CPN-Based IWS

A CPN-based IWS will be adopted in this study due to the imbalanced CPN/WSN architecture of a simple star (Fig. 1). In a single WBAN, the CPN plays the role of the master and the WSNs are the slaves. The CPN manages the join, leave, and functional-control of the WSNs. In contrast, WSNs are passive devices, which are designed to retrieve specific vital signals such as blood pressure or electrocardiograms (ECG)

Random Incomplete Coloring:

Given $G=(V,E)$, $u \in V$; $C_u(r)$ is the set of available colors of u in coloring round r. The initial size of the available color set is $|C_u(0)| = k$. For each coloring cycle:

While u is uncolored,

1. u chooses a color c_u from $C_u(r)$ with a random value, $\Re_u$.
2. u broadcasts its RVC message including c_u and $\Re_u$ to $N(u)$.
3. If u receives RVC messages from $v \in N(u)$ with $\Re_v \geq \Re_u$ and $c_v = c_u$, u remains uncolored. Otherwise, u is colored by c_u. (***Random value coloring***)
4. if u wins the color, it broadcasts the color taken notification.
5. u removes the colors taken by $N(u)$ from $C_u(r+1)$.
6. If $|C_u(r+1)| = 0$, u becomes uncolored. (***Incomplete coloring***)

Fig. 4. Random incomplete coloring.

and forwarding them to the CPN. Besides, a CPN is most likely to be embedded in personal devices such as cellular phones or PDAs with larger and rechargeable batteries. In contrast, a WSN is expected to be lightweight (small battery) and even nonrechargeable for certain implantable applications. These two unbalanced features suggest shifting power-consuming network controls from WSNs to the CPN. Thus, a CPN-based two-step IWS, which is illustrated in Fig. 3, is assumed in this study. The CPN first negotiates the WBAN resources with other CPNs that are in the mutually interfering range. The CPN then assigns reserved resources to its WSNs. As a result, the WSN wakes up only when 1) receiving beacon messages carrying the preregularized transmission schedule from the associated CPN and 2) transmitting vital signals following the schedule to that CPN.

The CPN-based IWS can now be modeled as a unit-disk graph coloring problem. A 2D randomly constructed graph (in short, random graph) $G = (V, E)$ is generated to model the WBAN network. $V(G)$ represents the set of CPNs; $E(G)$ represents the set of conflict links between CPNs. The first step in generating the graph is to randomly deploy $n = |V(G)|$ vertices in a field to simulate the random positions[3] of WBAN users. Consequently, edges are added to connect vertices if the distance between CPNs is equal to or less than the mutually interfering range between WBANs (the radius of the unit-disk). In this sense, the graph of CPN-based IWS is similar to that of MANET scheduling. However, they have different resource scheduling strategies. In MANET, each vertex represents a wireless node. MANET focuses on efficient internode communication and routing. Hence,

3. In some cases, waiting lines, for example, user positions follow certain rules instead of random deployments, which yield special graphs such as lines or grids. Although these graphs might reflect more real scenarios in our life than the random graph does, they need more complicated analysis skills due to their restrictions of graph formation. Therefore, to make the discussion of the proposed RIC more intuitive, this study focuses on the performance analysis of the random graph.

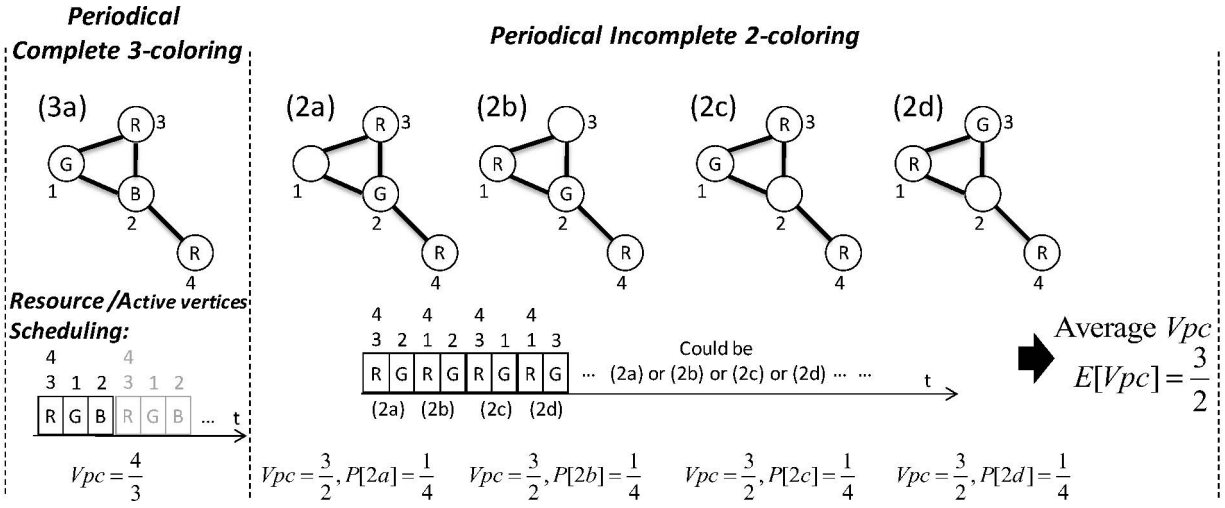

Fig. 5. Periodical complete and incomplete coloring (colors R,G,B are swappable).

"edge" coloring, which models the scheduling of "node-to-node communications," can be adopted. In contrast, in CPN-based IWS, each vertex represents a sensor group (WBAN). CPN-based IWS tries to resolve the interference between sensor groups belonging to different users. Therefore, "vertex" coloring, which models the scheduling of active "CPN-based sensor groups," is appropriate. As a result, for CPN-based IWS, a k-coloring of the random graph is labeled $V(G) \rightarrow C$, where $|C| = k$, such that adjacent vertices receive distinct colors. The labels are colors, which are mapped to different resource units for associated data transmissions (WSNs to the CPN). Only k resource mappings can be decided when a k-coloring algorithm is executed once. We assume that every WSN always has data to be transmitted to the CPN. Hence, the coloring is periodically performed to map wireless resources to all these data transmissions. The target of this study is to devise a coloring method that simultaneously satisfies two IWS requirements: 1) low time-complexity and 2) high spatial reuse.

3 Random Incomplete Coloring

The proposed random incomplete coloring has two major components: 1) a proposed random-value coloring method and 2) a proposed incomplete coloring approach. The random value coloring is a low time-complexity coloring method, which is designed for quick IWS. On the other hand, incomplete coloring is a high spatial-reuse coloring approach, which modifies the conventional coloring rule to explore the potential high spatial reuse when $k < \chi(G)$.

3.1 Random Value Coloring

Random value coloring is a method that realizes oriented coloring. It overcomes two major problems of oriented coloring [18]: fairness and oriented conflict-circle (deadlock circle), as outlined in Section 2.1. The method of random value coloring is to adopt a random value comparison to generate instant priority differences between all adjacent vertices, as illustrated in Fig. 4 (except Step 6 for the incomplete coloring).

In Fig. 4, the fairness of random value coloring can be supported if the random values $\Re$ from different vertices are generated with an identical uniform distribution.[4] Due to the symmetry between vertices, it is obvious that the probability that a vertex generates the maximum random value (wins the color) among $(n-1)$ competitors is $1/n$, where "competitors" means adjacent vertices contending for the same color. Thus, each vertex has equal radio resource sharing with its adjacent vertices. Besides, the way that random value coloring avoids an oriented conflict circle can easily be observed, since it is not possible to have the ordering of the random values of vertices in a circle with a one-way orientation $\Re_{v1} > \Re_{v2} > \cdots > \Re_{vn} > \Re_{v1}$. The fairness and deadlock-circle-free properties of the proposed method makes oriented coloring possible to realize for quick IWS.

3.2 Incomplete Coloring

Incomplete coloring improves spatial reuse by greedily coloring a graph with $k < \chi(G)$. Normally, it is not possible to completely color a graph using $k < \chi(G)$ colors because color conflict is unavoidable and cannot be resolved.[5] Thus, incomplete coloring allows uncolored vertices to avoid conflict when vertices run out of k colors, as illustrated at Step 6 of Fig. 4. Note that when applying incomplete coloring to IWS, the uncolored node means a CPN reserves no resource in that coloring. The WBAN of this CPN becomes temporarily inactive and generates no interference with its neighbor WBANs. The example in Fig. 5 demonstrates how incomplete coloring improves spatial reuse (on average).

Definition 3.1. *Vertices-per-color (*Vpc*), which is defined as the average number of vertices colored by each color, is used to evaluate the average spatial reuse (color reuse) of periodical coloring. Higher* Vpc *implies more wireless nodes can*

4. $f(x) = 1/(b-a), a \le x \le b$; otherwise, $f(x) = 0$.

5. Assume $k < \chi(G)$ and G can be completely colored by k colors (adjacent vertices receive distinct colors). However, $\chi(G)$ is defined as the minimum colors to completely color G and thus $k \ge \chi(G)$ contradicts $k < \chi(G)$. As a result, there must be adjacent vertices that receive the same color.

simultaneously transmit packets using the same resource unit (color), that is, the system has higher spatial reuse on average.

Definition 3.2. *A coloring round is defined as the execution of all steps in the while loop of the coloring algorithm (e.g., Steps 1 to 6 in Fig. 4). A coloring cycle is defined as the execution of all the coloring rounds required to leave the while loop, that is, the end of the algorithm.*

Graph G with four vertices in Fig. 5 can be completely colored by $\chi(G) = 3$ colors (case 3a), written φ_3. Thus, $Vpc(\varphi_3) = 4/3$. On the other hand, if two colors are used for incomplete coloring ($k = 2$), written $\varphi\prime_2$, there are four possible results at the end of the coloring cycle: 2a to 2d. Because 2a to 2d all have three vertices colored by two colors, 2a to 2d have identical $Vpc = 3/2$. The probability that each case happens depends on the color contention scheme. Assume a random value coloring method is adopted. Because cases 2a to 2d are symmetric and vertices 1 to 4 have equal priority in the contention, each case has an identical $1/4$ probability of showing up. As a result, when the incomplete coloring with $k = 2$, $\varphi\prime_2$, is iteratively performed, $E[Vpc(\phi\prime_2)] = 3/2$ for each coloring cycle. There is an increase of 12.5 percent over $Vpc(\varphi_3) = 4/3$ on average.

Of course, the three-color complete coloring schedules one more resource than the two-color incomplete coloring in each coloring cycle. In periodical coloring, to schedule the same number of resources, a k-color incomplete coloring ($k < \chi(G)$) needs $\chi(G)/k$ times more coloring cycles than that of a $\chi(G)$-color complete coloring, which increases the exchange of coloring messages required for periodical coloring. This could affect the collision probability of coloring messages in a practical IWS implementation. The tradeoffs between spatial reuse and affordable coloring-message exchanges will be closely analyzed in Section 5.

4 Analytical Model of Random Value and Incomplete Coloring

4.1 Upper Bound of the Time and Bit Complexity of RIC

With the proposed random value coloring method, the time-complexity of RIC can be further decreased from $\tilde{O}(\sqrt{\log n})$ [18] to $O(e^{W(2\ln n)/2})$, where $W(x)$ is the Lambert W function [20]. The time-complexity (upper bound) of RIC to color a graph with a constant-degree Δ is calculated. This could be used to observe the time-complexity of the 2D topology model. Because vertices are randomly deployed in the 2D model, every vertex should have a similar vertex degree. The accuracy of this constant-degree assumption will be verified in the Section 5.1.

Definition 4.1. *Oriented conflict path is defined as a path with all edges having a one-way orientation and all vertices in this path contending for the same color.*

Lemma 4.2. *A graph having the longest OCP with l-length (l-vertices) can be colored in at most l rounds.*

This lemma is proved by [18], which shows that, in each coloring round, at least one vertex can be colored in the OCP. Thus, a graph with an l-length OCP can be colored within l rounds.

Lemma 4.3. *The probability that an OCP has length larger than or equal to i in round r of the RIC algorithm is less than or equal to $((\frac{1}{k})^{i-1} \cdot \frac{1}{i!})^r$.*

For the RIC algorithm, an OCP is only generated when the random values of vertices in the path are in descending order, $\Re_{v1} > \Re_{v2} > \Re_{v3} > \cdots$ (Definition 4.1). Therefore, the probability that an OCP has length larger than or equal to i can be expressed as

$$\begin{aligned} & k\left(\frac{1}{k}\right)^i \cdot P[\Re_{v1} > \Re_{v2} > \cdots > \Re_{vi}] \\ &= k\left(\frac{1}{k}\right)^i \cdot \prod_{m=1}^{i} P[\Re_{vm} = Max\{\Re_{vn}, n \in [m,i]\}] \\ &= k\left(\frac{1}{k}\right)^i \cdot \prod_{m=1}^{i} \frac{1}{m} \text{ (Due to the symmetry of } \Re_{vm}) \\ &= k\left(\frac{1}{k}\right)^i \cdot \frac{1}{i!} = \left(\frac{1}{k}\right)^{i-1} \cdot \frac{1}{i!}, \end{aligned} \tag{1}$$

where k is the number of colors used in the RIC. The length of the OCP can only decrease or stay the same during the coloring. Hence, to make sure the length of an OCP is larger than or equal to i in round r, the length of this OCP should always be larger than or equal to i from rounds 1 to r. Therefore, the probability that an OCP has length larger than or equal to i in round r is less than or equal to $((\frac{1}{k})^{i-1} \cdot \frac{1}{i!})^r$.

Theorem 4.4. *Given a graph with n vertices and constant degree Δ, the time-complexity of the RIC algorithm for any number of colors is $O(e^{W(2\ln n)/2})$ rounds, where $W(x)$ is the Lambert W function.*

Proof. A two-phase analysis, which is similar to [18], [21] is adopted to calculate the time-complexity of the proposed RIC algorithm. Phase I lasts from the first coloring round to r_Γth, $r_\Gamma = 10e^{W(2\ln n)/2}$ rounds; Phase II lasts from $(r_\Gamma + 1)$th rounds to the end of the coloring cycle. A graph may contain multiple OCPs during the coloring. At the end of Phase I, we prove that the length of any OCP of the graph will be confined by the length $l_\Gamma = e^{W(2\ln n)/2}$ with a high probability. According to **Lemma 4.2**, this graph can be further colored with at most $e^{W(2\ln n)/2}$ coloring rounds in Phase II. Thus, the total coloring rounds can be proved to be $O(10e^{W(2\ln n)/2}) + O(e^{W(2\ln n)/2}) = O(e^{W(2\ln n)/2})$. □

At the end of Phase I, the length of any OCP will be proven to be confined by the length $l_\Gamma = e^{W(2\ln n)/2}$ with a high probability. This can be a dual proof: there is a low probability that at least one OCP of the graph is of length larger than l_Γ at the end of Phase I. This probability is denoted as $P[\mathbb{E}]$. The probability of an OCP in such event is denoted as $P[l(r_\Gamma) > l_\Gamma]$, where $l(r_\Gamma)$ is the length of the OCP in round r_Γ. Also, in a graph with n vertices, $n\Delta^i$ is the maximum[6] number of OCPs with length i. Therefore,

6. Because each OCP could start from any of n vertices. Also, each vertex has Δ adjacent vertices in the constant Δ degree graph, so there are Δ^i possible combinations to generate an OCP with length i.

$$\begin{aligned} P[\mathbb{E}] &\le \sum_{i=l_\Gamma+1}^{n} n\Delta^i \cdot P[l(r_\Gamma)=i] \\ &\le \sum_{i=l_\Gamma+1}^{n} n\Delta^i \cdot P[l(r_\Gamma)\ge i] \\ &\le \sum_{i=l_\Gamma+1}^{n} n\Delta^i \cdot \left(\left(\frac{1}{k}\right)^{i-1}\cdot\frac{1}{i!}\right)^{r_\Gamma} \text{(Lemma 4.3)}. \end{aligned} \tag{2}$$

For simplicity in the following calculation, the approximation of the factorial term, $i! \ge e(\frac{i}{e})^i$, is applied. Thus, $\sum_{i=l_\Gamma+1}^{n} n\Delta^i \cdot ((\frac{1}{k})^{i-1}\cdot\frac{1}{i!})^{r_\Gamma} \le \sum_{i=l_\Gamma+1}^{n} n\Delta^i \cdot ((\frac{1}{k})^{i-1}\cdot\frac{1}{e(i/e)^i})^{r_\Gamma}$. Each term in the summation can be simplified to

$$n\Delta^i \cdot \left(\frac{k^{10}}{e^{10}}\right)^{l_\Gamma}\left(\frac{e^{10}}{k^{10}}\right)^{i\cdot l_\Gamma}\frac{1}{(i^{i\cdot l_\Gamma})^{10}},$$

which is less than or equal to $\frac{n}{(i^{i\cdot l_\Gamma})^7}$ due to $i^{i\cdot l_\Gamma} > O(1)^{i\cdot l_\Gamma} > O(1)^i > O(1)^{l_\Gamma}$(recall that $i > l_\Gamma$). Also,

$$\frac{n}{(i^{i\cdot l_\Gamma})^7} \le \frac{n}{(l_\Gamma^{l_\Gamma^2})^7}$$

and $l_\Gamma = e^{W(2\ln n)/W(2\ln n)22}$ lead to $n = l_\Gamma^{l_\Gamma^2}$ (recall that $z = W(z)\exp[W(z)]$, for any complex number z). Therefore,

$$P[\mathbb{E}] \le \sum_{i=l_\Gamma+1}^{n}\frac{n}{n^7} \le \frac{1}{n^5},$$

which approaches 0 as $n \to \infty$. As a result, at the end of Phase I, the lengths of any OCPs confined by $l_\Gamma = e^{W(2\ln n)/2}$ are proved with a high probability. The upper bound of total rounds that the RIC algorithm requires is the summation of the maximum rounds of Phases I and II, $O(10e^{W(2\ln n)/2}) + O(e^{W(2\ln n)/2}) = O(e^{W(2\ln n)/2})$, Q.E.D.

Definition 4.5. *As is explained in [19], the bit complexity of a distributed algorithm (per channel) is defined as the total number of bits exchanged (per channel) during its execution.*

Theorem 4.6. *The bit complexity of the RIC algorithm is* $O(e^{W(2\ln n)/2}\log n)$.

In each coloring round of the RIC algorithm, each vertex exchanges one random number and one color identification with each neighbor on each channel. We assume the random number has finite resolution and hence can be expressed by bits with a constant bit length C. Also, the necessary colors for a n-vertices-graph coloring can always be identified by $O(\log n)$ bits. As a result, for the RIC, the number of bits exchanged in a coloring cycle ($O(e^{W(2\ln n)/2})$ rounds) is $O(e^{W(2\ln n)/2}\log n)$.

4.2 Spatial Reuse of Incomplete Coloring

Similar to the time-complexity analysis, the Vpc of RIC for a constant degree Δ graph is calculated. P_c is defined as the probability that a vertex can be colored by RIC. In the constant degree graph, the P_cs of all vertices are identical due to the symmetric graph structure. Each k coloring decides a k-color vertex-to-color mapping. Thus, $Vpc = n\frac{P_c}{k}$, where n is the number of vertices in the graph. Consequently, to calculate the Vpc, all we need to know is the value of P_c.

Theorem 4.7. *For a graph with constant degree* Δ*, the probability that each vertex can be colored by the algorithm RIC, written as* P_c*, is satisfied by the equation*

$$P_c = \sum_{i=1}^{k}(-1)^{i-1}\binom{k}{i}\left(1-i\frac{P_c}{k}\right)^{\Delta}.$$

Proof. The idea of the P_c calculation is based on the probability complementary between each vertex and its adjacent vertices. In RIC, the probability that a vertex can be colored is $P_c = \sum_{i=1}^{k} P_{c_i}$, where P_{c_i} represents the probability that the vertex is colored by color c_i. If a vertex can be colored, its adjacent vertices must have the color combinations without using c_1 or c_2 or $\cdots$ or c_k, written $P[\bigcup_{i=1}^{k}\overline{c_i}]$, where $\overline{c_i}$ denotes that adjacent vertices are not colored by c_i. Thus, $P_c = \sum_{i=1}^{k} P_{c_i} = P[\bigcup_{i=1}^{k}\overline{c_i}]$, which can be expressed as

$$\begin{aligned} P\left[\bigcup_{i=1}^{k}\overline{c_i}\right] &= \sum_{i=1}^{k} P[\overline{c_i}] - \sum_{i,j:1\le i<j\le k} P\left[\overline{c_i}\cap\overline{c_j}\right] \\ &\quad + \sum_{i,j,l:1\le i<j<l\le k} P\left[\overline{c_i}\cap\overline{c_j}\cap\overline{c_l}\right] \\ &\quad - \cdots + (-1)^{k-1}P[\overline{c_1}\cap\cdots\cap\overline{c_k}] \\ &= \sum_{i=1}^{k}(1-P_{c_i})^{\Delta} - \sum_{i,j:1\le i<j\le k}(1-P_{c_i}-P_{c_j})^{\Delta} \\ &\quad + \sum_{i,j,l:1\le i<j<l\le k}(1-P_{c_i}-P_{c_j}-P_{c_l})^{\Delta} \\ &\quad - \cdots + (-1)^{k-1}(1-P_{c_1}-\cdots-P_{c_k})^{\Delta}. \end{aligned} \tag{3}$$

Due to the symmetry of each color in the equation, $P_{c_1} = P_{c_2} = \cdots = P_{c_k} = \frac{P_c}{k}$, thus

$$P_c = \sum_{i=1}^{k}(-1)^{i-1}\binom{k}{i}\left(1-i\frac{P_c}{k}\right)^{\Delta}. \tag{4}$$

As a result, P_c can be obtained by solving for the real root of (4). □

5 Computer Simulation

A two-stage performance evaluation of RIC is provided in this section. The first stage evaluates the time-complexity and spatial reuse of the RIC. At the second stage, RIC is applied in an IWS with a TDMA framing structure, a common structure used in sensor or body area networks [2]. It tests the convergence speed and channel utilization of IWS in mobile WBAN scenarios. Packet collisions of data packets and coloring messages will be considered in the second stage.

5.1 Performance Evaluation of RIC

Two-dimensional random graphs with various vertex densities are used to evaluate the performance of the RIC. Following the system model in Section 2, n vertices are randomly deployed in a $10 \times 10\ m^2$ square. The mutually interfering range is set as 2 m. n can be 12, 25, 50, 100 to simulate low, middle, high, and extremely high densities. The performance metrics used to evaluate time-complexity and spatial reuse of coloring are rounds-per-cycle (Rpc) and

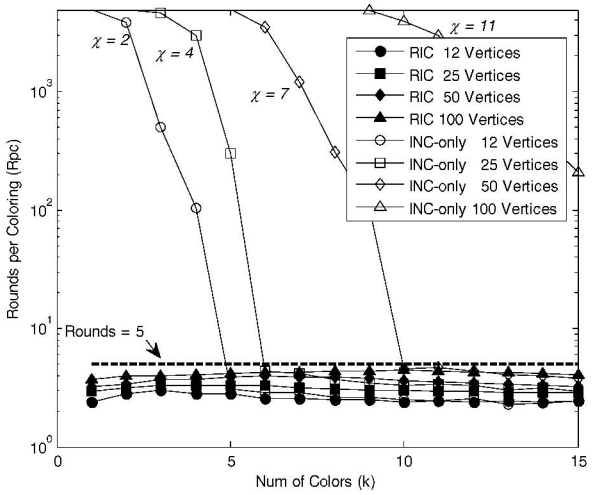

Fig. 6. Rounds per coloring cycle of RIC and INC-only.

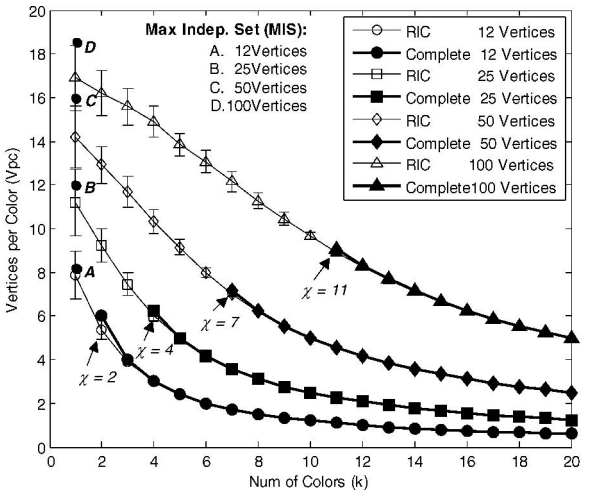

Fig. 8. Vertices-per-color of RIC and complete colorings.

vertices-per-color, respectively. Rpc is defined as the total coloring rounds required to finish a coloring cycle.

Fig. 6 compares the Rpc of the proposed RIC with INC-only. INC-only is an incomplete coloring combined with nonoriented coloring [17]. Due to the low time-complexity of the RIC, $O(e^{W(2\ln n)/2})$, Fig. 6 shows that RIC can be finished within five rounds in any number of colors (1∼15 colors) and vertex densities (12∼100 vertices). In contrast, the coloring rounds of INC-only dramatically increase, especially when the vertex density is high or few colors are used. This huge difference comes from the different strategies of RIC and INC-only in dealing with color conflict. RIC forces each color conflict to generate a winner. On the other hand, for INC-only, vertices in the conflict pair both give up the conflict color and reselect new colors in the next coloring round, which prolongs the coloring time. The time-complexity of INC-only grows significantly in the few k (reduced color choices) or the high density (increasing competitors) scenarios.

For the spatial reuse analysis of RIC, Fig. 7 compares the analytical model (Theorem 4.7 based on the constant-degree graph assumption) with simulation results for RIC in a 2D random graph. Fig. 7 shows that the analytical model can correctly predict the Vpc of RIC, which monotonously increases while the number of colors k decreases.

Fig. 8 compares the Vpc of RIC with complete coloring [16], [17], [18]. Unlike RIC that keeps improving Vpc following the decrease of colors, the improvement of complete coloring stops at $\chi(G)$ colors, which are the minimum colors it can use. The Vpc of RIC has an increase of 90 percent over the complete coloring using $\chi(G)$ colors when the WBAN density is larger than the middle density (25 vertices) and the coloring number is 1. Another comparison with RIC in Fig. 8 is the optimum Vpc in one coloring, which is a dual problem of finding the maximum independent set (MIS)[7] in the given graph. Fig. 8 shows that RIC has near optimum Vpc at low and middle densities (12 and 25 vertices). Even at high and extremely high densities (50 and 100 vertices), RIC has a performance of around 90 percent compared with the MIS values.

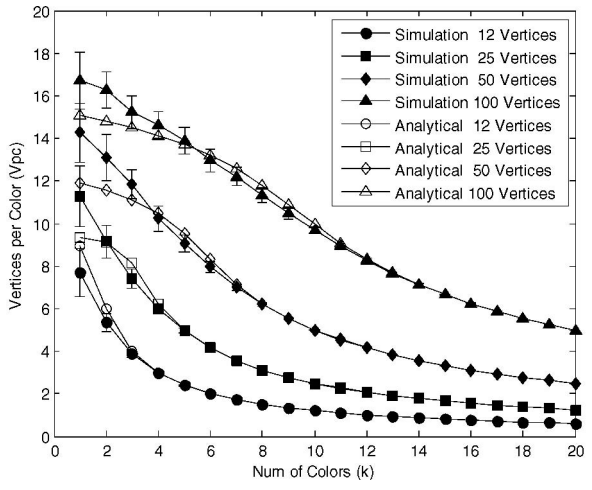

Fig. 7. Vertices-per-color of analytical model and simulations of RIC.

5.2 Performance Evaluation of CPN-Based IWS

Consequently, RIC is applied in a CPN-based IWS to observe how its high coloring speed and high spatial reuse improve IWS performance in mobile and dense WBAN scenarios.

5.2.1 Simulation Settings of Coloring-Based IWS

A proposed CPN-based IWS adopts a time-division multiple access with two distinct communication channels: inter and intra-WBAN channels. It helps to realize and compare different kinds of coloring-based IWSs. A CPN uses both channels for inter-WBAN resource contention and intra-WBAN data (vital signals) collection, respectively; a WSN only uses an intra-WBAN channel for data (vital signals) transmission. Following the steps of a CPN-based IWS in Section 2, a CPN first uses the inter-WBAN channel to contend time slots through a coloring algorithm. The CPN then sends a beacon through an intra-WBAN channel to allocate obtained time slots to its WSN. Finally, the WSN transmits a data packet to its associated CPN through the

7. Maximum Independent Set is defined as the maximum set of pairwise nonadjacent vertices in a graph.

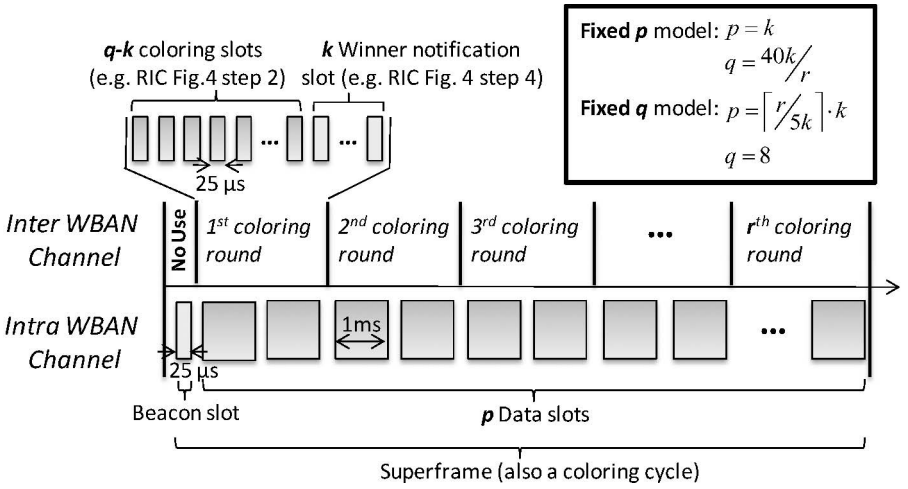

Fig. 9. Superframe for coloring-based IWS.

intra-WBAN channel at the time slot that was prescheduled by the CPN.

The framing structure is illustrated in Fig. 9. A coloring cycle is performed for each superframe. The intra-WBAN channel consists of one beacon slot and p data slots. Each CPN can reserve at most one slot after each coloring cycle. The number of data slots to be scheduled in each coloring cycle is set as k (equals to the number of colors used in the coloring). The duration of each data slot is 1 ms. On the other hand, the inter-WBAN channel consists of r slot-groups for r coloring rounds in a cycle. Each coloring round has q slots and is subdivided into $(q-k)$ coloring slots and k winner notification slots, where k is the number of colors used for coloring. Coloring slots are used for exchanging coloring messages between CPNs (e.g., Fig. 4 Step 2). The CPN chooses a coloring slot in each coloring round to transmit its coloring message. The coloring slot is randomly chosen to reduce potential collisions between coloring messages. Once a CPN wins the slot (color), it broadcasts the winner message at the associated winner notification slot (e.g., Fig. 4 Step 4). Because the coloring message exchanged across the inter-WBAN channel contains only color and random value information, the duration of coloring and winner notification slots are set as 25 μs, which is $1/40$ of the data slot at the intra-WBAN channel. In this study, we skip the steps of superframe synchronization between CPNs, which is beyond the scope of this study. Related work on superframe synchronization can be found in [22].

The settings of p (number of data slots in a superframe) and q (number of coloring slots in a coloring round) are two important control variables that dominate two kinds of data collision: 1) out-of-date scheduling and 2) ill scheduling. Out-of-date scheduling happens when the frequency of the IWS cannot catch up to the frequency of topology changes due to user mobility. The data transmissions of WSNs scheduled by the out-of-date scheduling might collide with other transmissions from unnegotiated WBANs. Because IWS is performed for each superframe, such collisions are dominated by the duration of the superframe p. The second kind of collision is caused by ill scheduling, which results from the collision of coloring messages (in short, coloring collision) while CPNs broadcast their coloring messages in the same coloring slot. Without correctly receiving coloring messages from adjacent CPNs, a CPN could make a mistake on treating itself as the slot (color) winner. As a result, data transmissions of WSNs belonging to different WBANs could be scheduled to the same data slot and then collide with each other. Since coloring slots are randomly chosen by each CPN, the larger the number of coloring slots, the lower the collision rate. The number of coloring slots is decided by the value q. To closely study both kinds of collisions, two types of settings are used: fixed-p and fixed-q. For the fixed-p model, p is set as the number of colors k (coloring numbers). Thus, each coloring round at the inter-WBAN channel has $q = 1\ \mathrm{ms}/25\ \mu\mathrm{s.k/r} = 40\mathrm{k/r}$, where r is the number of coloring rounds. As for the fixed-q model, we choose $(k, r) = (1, 5)$ to set the baseline size of q as eight slots, which introduces the most serious coloring-message collision[8] of φ_{RV-INC}. Thus, $p = 8r/40 = r/5$. Because each k coloring provides k slots scheduling, it is more convenient to make p an integral multiple of k. As a result, p is modified as $\lceil \frac{r}{5k} \rceil k$ and the coloring result repeats every k slots.

The generation of mobile WBAN topology is similar to the 2D random graph. The initial positions of n WBANs are randomly located in a $10 \times 10\ \mathrm{m}^2$ square. n can be 12, 25, 50, 100 to simulate low, middle, high, and extremely high WBAN densities. The mutually interfering range of WBANs is set as 2 m. Also, to simulate WBAN mobility, the location change of WBANs follows the Gauss-Markov mobility model [23]. We use study in [23] to simulate the smooth movement path of a human, while avoiding the sudden stops and sharp turns that happen in the random walk mobility model [24]. The Gauss-Markov mobility model has a tuning factor α to control the randomness of WBAN movement. α is set as 0.3 in this study ($\alpha = 0$ and $\alpha = 1$ correspond to Brownian motion and linear motion, respectively).

System throughput is the performance index used to evaluate IWS. Without loss of generality, system throughput is defined as effective transmissions per slot (Tps),

8. Fig. 6, RIC can be finished within five rounds ($r = 5$). While $r = 5, k = 1$ is the setting that yields a minimum q from the equation $q = 40k/r$, which introduces the most serious coloring-message collision.

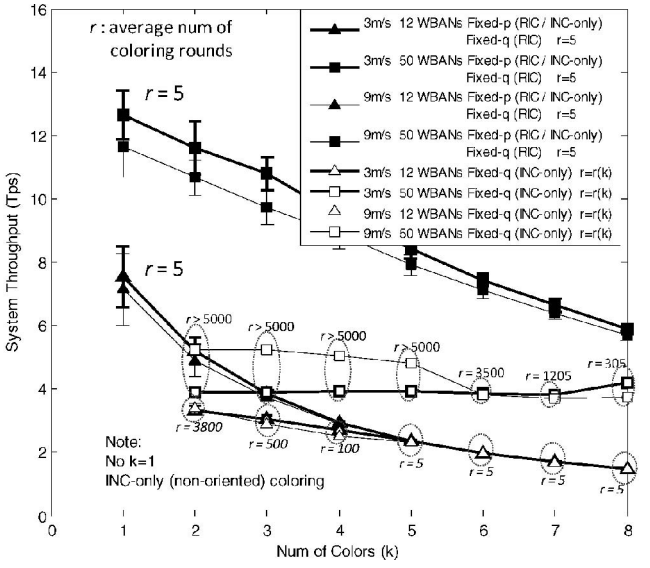

Fig. 10. Transmission per slot of IWS (ignoring ill scheduling).

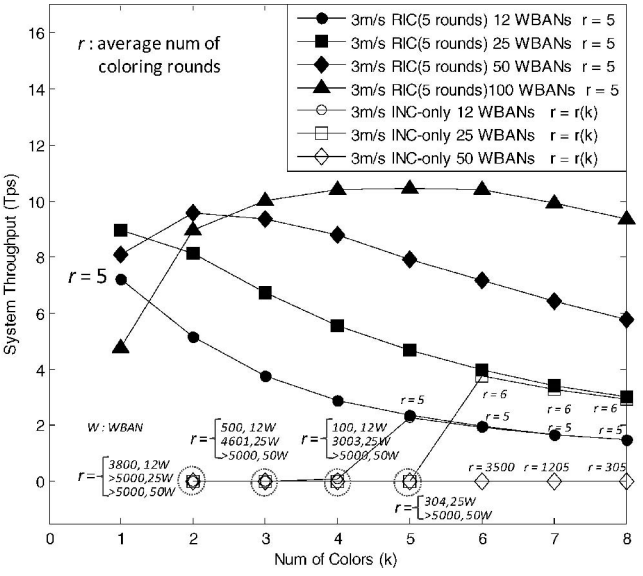

Fig. 11. System throughput of IWS with the fixed-p model.

which counts data transmissions of all WSNs that are actually received by CPNs in the system. Tps is similar to the vertex-per-color (Vpc) but further considers performance degradation caused by data collision.

5.2.2 System Throughput of IWS

Coloring speed is found to be the key factor that affects the performance of IWS. Fig. 10 compares the system throughput of IWS using the RIC and INC-only algorithms. INC-only can perform sub-$\chi(G)$ coloring but has a much higher time-complexity than RIC (see Fig. 6). First, in Fig. 10, ill scheduling is temporarily ignored to make the observation of out-of-date scheduling much more clear. Because the collisions of coloring messages are ignored, the performances of RIC and INC-only in the fixed-p model are identical. Also, $r_{RIC} = 5$ leads to $p_{RIC} = k$, which makes the performance of RIC in fixed-p and fixed-q models equivalent. Fig. 10 shows that the fixed-p model overcomes the mobility much better than the fixed-q model. In the fixed-q model, $p_{INC-only} = \lceil \frac{r}{5k} \rceil k$ is prolonged by the high time-complexity (high number of r) of INC-only and thus fails to respond in a timely fashion to topology changes. On the other hand, in the fixed-p model, $p = k$ is independent of coloring rounds r. Throughput is only slightly degraded while mobility is increased from 3 to 9 m/s. Furthermore, in the fixed-p model, throughput is improved while the coloring number k is decreased. This improved throughput ought to lead to more out-of-date scheduling. Fortunately, the frequency of IWS is inversely proportional to the duration of the superframe $(k+1)$. Decreasing k increases IWS frequency to compensate for the collisions caused by throughput improvement.

Now, we focus on the fixed-p model. Ill scheduling (coloring collision) is found to be the major factor that seriously degrades the performance of IWS. Fig. 11 illustrates the system throughput of IWS in the fixed-p model after considering both out-of-date and ill-scheduling collisions. It shows that RIC has a much higher Tps than INC-only. The reason comes from the substantially fewer coloring rounds of RIC than that of INC-only. $r_{INC-only}$ might be larger than thousands of slots due to the inefficient recoloring of INC-only, which makes $q_{INC-only}$ much lower than q_{RIC} ($q = 40k/r$) and introduces serious collisions of coloring messages. For INC-only, $q = 40k/r(k)$ can be increased by increasing k and decreasing $r(k)$ (coloring rounds $r(k)$ decrease while color choices k increase, as shown in Fig. 6). The coloring collision of INC-only is relieved when k is larger than 4 and 5 for the scenarios of 12 and 25 WBANs, respectively. However, increasing k also decreases Tps (referring to the decreasing Vpc in Fig. 7). For RIC, the tradeoff between coloring collision and Tps reduction yields optimum throughputs when k is 2 and 5 (instead of 1) for the 50 and 100 WBANs cases, respectively.

6 Conclusion

In this work, random incomplete coloring is proposed to realize a fast and high spatial-reuse inter-WBAN scheduling. Unlike conventional complete coloring schemes, RIC is not limited by the tradeoff between coloring speed and spatial reuse. RIC can always provide fast convergence with time-complexity $O(e^{W(2\ln n)/2})$ in any spatial reuse requirement. Furthermore, RIC can support an increase of up to 90 percent of spatial reuse over the conventional complete coloring using chromatic $\chi(G)$-colors, which is known to be the optimal coloring of complete coloring. In the simulation, RIC is applied in a CPN-based IWS protocol with TDMA framing structure. Simulation results show that RIC does overcome inter-WBAN collisions and thus provides high system throughput for mobile wireless body area networks.

This study focuses on the scenario of random-user position, which is modeled as a 2D random graph. In the future, we would like to analyze the performance of RIC in other special scenarios. For example, users in a waiting line, a movie theater, or a coffee bar. These scenarios can be modeled as a line, a grid, and a clustered graph, respectively. Also, in our future work, we will try to relax the strict assumptions made in this paper, such as perfect superframe synchronization. We will implement RIC in a mote-base

WBAN to evaluate its real-world performance and make comparisons with existing WBAN solutions, IEEE 802.15.4 and Bluetooth networks.

ACKNOWLEDGMENTS

The authors greatly thank Prof. Hung-Lin Fu for the help and suggestions on the coloring algorithm and Hung-Hui Juan for the reviewing. They also want to thank NSC of Taiwan for the support of this project, which is under Grant NSC100-2220-E-009-016.

REFERENCES

[1] M. Patel and W. Jianfeng, "Applications, Challenges, and Prospective in Emerging Body Area Networking Technologies," *IEEE Wireless Comm.,* vol. 17, no. 1, pp. 80-88, Feb. 2010.
[2] M. Chen, S. Gonzalez, A. Vasilakos, H. Cao, and V.C. Leung, "Body Area Networks: A Survey," *Mobile Networks and Applications,* vol. 16, no. 2, pp. 171-193, 2011.
[3] I.F. Akyildiz, W.L. Su, Y. Sankarasubramaniam, and E. Cayirci, "A Survey on Sensor Networks," *IEEE Comm. Magazine,* vol. 40, no. 8, pp. 102-114, Aug. 2002.
[4] S.M. Jiang, Y.D. Liu, Y.M. Jiang, and Q.G. Yin, "Provisioning of Adaptability to Variable Topologies for Routing Schemes in MANETs," *IEEE J. Selected Areas in Comm.,* vol. 22, no. 7, pp. 1347-1356, Sept. 2004.
[5] B. De Silva, A. Natarajan, and M. Motani, "Inter-User Interference in Body Sensor Networks: Preliminary Investigation and An Infrastructure-Based Solution," *Proc. Sixth Int'l Workshop Wearable and Implantable Body Sensor Networks,* pp. 35-40, 2009.
[6] S.H. Cheng and C.Y. Huang, "Power Model for Wireless Body Area Network," *Proc. IEEE Biomedical Circuits and Systems Conf.,* pp. 1-4, 2008.
[7] S.H. Cheng, M.L. Liu, and C.Y. Huang, "Radar Based Network Merging for Low Power Mobile Wireless Body Area Network," *Proc. Fourth Int'l Symp. Medical Information and Comm. Technology,* 2010.
[8] I. Howitt, "Mutual Interference between Independent Bluetooth Piconets," *IEEE Trans. Vehicular Technology,* vol. 52, no. 3, pp. 708-718, May 2003.
[9] A. El-Hoiydi, "Interference between Bluetooth Networks - Upper Bound on the Packet Error Rate," *IEEE Comm. Letters,* vol. 5, no. 6, pp. 245-247, June 2001.
[10] S. Gandham, M. Dawande, and R. Prakash, "Link Scheduling in Wireless Sensor Networks: Distributed Edge-Coloring Revisited," *J. Parallel and Distributed Computing,* vol. 68, no. 8, pp. 1122-1134, Aug. 2008.
[11] B.J.B. Fonseca Jr., "An Augmented Graph-Based Coloring Scheme to Derive Upper Bounds for the Performance of Distributed Schedulers in CSMA-Based Mobile Ad Hoc Networks," *Proc. Int'l Wireless Comm. and Mobile Computing Conf.,* pp. 761-766, 2006.
[12] S. Ramanathan, "A Unified Framework and Algorithm for Channel Assignment in Wireless Networks," *Wireless Networks,* vol. 5, no. 2, pp. 81-94, Mar. 1999.
[13] D.B. West, *Introduction to Graph Theory,* second ed. Prentice Hall, 2000.
[14] C. Zhu and M.S. Corson, "A Five-Phase Reservation Protocol (FPRP) for Mobile Ad Hoc Networks," *Wireless Networks,* vol. 7, no. 4, pp. 371-384, Aug. 2001.
[15] IEEE 802.15 WPAN Task Group 6 Body Area Networks, "15-08-0644-09-0006-tg6 Technical Requirements Document," 2008.
[16] A. Bjorklund, T. Husfeldt, and M. Koivisto, "Set Partitioning via Inclusion-Exclusion," *SIAM J. Computing,* vol. 39, no. 2, pp. 546-563, July 2009.
[17] Ö. Johansson, "Simple Distributed $\Delta + 1$-Coloring of Graphs," *Information Processing Letters,* vol. 70, no. 5, pp. 229-232, June 1999.
[18] K. Kothapalli, C. Scheideler, M. Onus, and C. Schindelhauer, "Distributed Coloring in O(Radic (log n)) Bit Rounds," *Proc. 20th Int'l Parallel and Distributed Processing Symp.,* p. 10, 2006.
[19] Y. Métivier, J.M. Robson, N. Saheb-Djahromi, and A. Zemmari, "About Randomised Distributed Graph Colouring and Graph Partition Algorithms," *Information and Computation,* vol. 208, no. 11, pp. 1296-1304, 2010.
[20] R.M. Corless, G.H. Gonnet, D.E.G. Hare, D.J. Jeffrey, and D.E. Knuth, "On the Lambert W Function," *Advances in Computational Math.,* vol. 5, pp. 329-359, 1996.
[21] D.A. Grable and A. Panconesi, "Nearly Optimal Distributed Edge Coloring in O(log log n) Rounds," *Random Structures & Algorithms,* vol. 10, no. 3, pp. 385-405, May 1997.
[22] C.T. Chou, J. Del Prado Pavon, and N. Sai Shankar, "Mobility Support Enhancements for the WiMedia UWB MAC Protocol," *Proc. Second Int'l Conf. Broadband Networks,* pp. 213-219, 2005.
[23] V. Tolety, "Load Reduction in Ad Hoc Networks Using Mobile Servers," master's thesis, Dept. of Math. and Computer Sciences, Colorado School of Mines, Colorado, 1999.
[24] T. Camp, J. Boleng, and V. Davies, "A Survey of Mobility Models for Ad Hoc Network Research," *Wireless Comm. & Mobile Computing,* vol. 2, no. 5, pp. 483-502, Aug. 2002.

Shih Heng Cheng received the bachelor's degree in electronics engineering from National Chiao Tung University (NCTU) in 2006. He is currently working toward the PhD degree in electronics engineering at NCTU. He got second position in the 2008 ARM Code-O-Rama microcontroller programming contest. His research interests currently include wireless sensor networks, ultralow power wireless body area networks, body channel models, telemedical platforms. He has two technical contributions in a standard meeting, IEEE 802.15 TG6 Wireless Body Area Network. Currently, he also has two patents pending. He is a student member of the IEEE.

Ching Yao Huang received the BS degree in physics from the National Taiwan University, Taiwan, in 1987 and the master's and PhD degrees in electrical and computer engineering from NJIT and Rutgers University (WINLAB), the state university of New Jersey, in 1991 and 1996, respectively. From 1996 to 2002, he was a system engineer (member of Technical Staff) at AT&T Whippany, New Jersey and then Lucent Technologies. In the years 2001 and 2002, he was an adjunct professor at Rutgers University and NJIT. Currently, he is with the Department of Electronics Engineering, National Chiao Tung University, Taiwan, and is an associate professor and the director of Technology Licensing Office and Incubation Center. He is the recipient of "Bell Labs Team Award" from Lucent in 2003, "Best Paper Award" from IEEE VTC Fall 2004, "Best Educator" from the Taiwan Ministry of Education, in 2007, and the "Outstanding Achievement Award" from the National Chiao Tung University in 2007. His research areas include medium access controls for cellular systems and wireless body area networks. He has published more than 70 technical memorandums, journal papers, and conference papers and is a chapter author in the book *Handbook of CDMA System Design, Engineering and Optimization*. Currently, he has 15 US patents and 20 pending patents and served as an editor/associate editor for ACM WINET and has Recent Patents on electrical engineering. He is a member of the IEEE.